Chemical Science

ROYAL SOCIETY OF CHEMISTRY

EDGE ARTICLE

View Article Online
View Journal | View Issue

Cite this: *Chem. Sci.*, 2025, **16**, 952

All publication charges for this article have been paid for by the Royal Society of Chemistry

Reversible formation of tetraphenylpentalene, a room temperature stable antiaromatic hydrocarbon†

Hugh J. Sanderson, [a] Andreas Helbig,[b] Gabriele Kociok-Köhn, [c] Holger Helten *[b] and Ulrich Hintermair *[a]

Received 23rd September 2024
Accepted 22nd November 2024

DOI: 10.1039/d4sc06439a

rsc.li/chemical-science

1,3,4,6-Tetraphenylpentalene (**Ph_4Pn**) has been synthesised by chemical oxidation of the corresponding pentalenide complex **Mg[Ph_4Pn]** with iodine. **Ph_4Pn** is a rare example of a room-temperature stable hydrocarbon that is antiaromatic by Hückel's rule and has been fully characterised by NMR and UV-vis spectroscopy, mass spectrometry as well as single-crystal X-ray diffraction. Quantum chemical studies including nucleus-independent chemical shift (NICS) and anisotropy of the induced current density (ACID) calculations showed the existence of an 8π antiaromatic core decorated with four independent 6π aromatic substituents. The formation of **Ph_4Pn** is reversible and it can be reduced back to the 10π aromatic **Ph_4Pn^{2-}** with potassium.

1. Introduction

Aromaticity, and by extension antiaromaticity, are core concepts in chemistry with different classifications.[1] The most familiar is Hückel aromaticity, embodied by the $4n + 2$ π-electron rule developed by Doering and Detert,[2] which is used for planar closed-shell monocyclic conjugated systems.[3] The opposite, Hückel antiaromaticity, is termed for molecules that have a $4n$ π-electron count yet satisfy the rest of the criteria.[4] Whereas aromaticity serves to provide a molecule with increased stability, antiaromaticity imparts destabilisation to the molecule along with other contrasting spectroscopic and magnetic properties (such as paratropic ring currents).[5,6] The concept of (anti)aromaticity was later extended to open-shell systems by Baird,[7] who showed that molecules with a $4n$ π-electron count display aromaticity in the triplet state whilst those with a formal $4n + 2$ π-electron count exhibit antiaromatic behaviour in the triplet state.[8] Other types of (anti)aromaticity have also been reported,[1] and mechanisms for electron delocalisation are known beyond π-conjugation.[9–13]

Compared to the interest in the different forms of aromaticity,[5] less attention has been paid to antiaromatic molecules and the properties they can possess. Hückel antiaromaticity can result in a lowering of the HOMO–LUMO gap[14] and the presence of a low-lying triplet state which may exhibit Baird aromaticity.[4,7,8,15,16] Thus, molecules possessing antiaromaticity have found use in areas such as optoelectronics, for example.[17–20] However, the destabilisation that arises from a fully conjugated $4n$ π-electron system often results in highly unstable molecules that react readily to relieve the antiaromatic strain – *e.g.* through dimerisation or by adoption of non-planar conformations.[21] The idea of concealed antiaromaticity has been proposed as a framework with which to identify the structural motifs used to stabilise antiaromatic systems, such that upon oxidation/reduction or photoexcitation aromatic systems may be formed.[22] Such motifs presented include sharing of 2π or 4π-electron fragments by a locally aromatic group to the $4n$ π-system and internal connections (*e.g.* C–C bonds) within the $4n$ π-system itself.

A classic example of a $4n$ π-system that alleviates, or conceals, its antiaromaticity is cyclooctatetraene (C_8H_8, **COT**) which adopts a non-planar boat conformation thus avoiding π-conjugation and formation of antiaromatic ring currents (Scheme 1). Pentalene (C_8H_6, **Pn**) is an 8 π-electron hydrocarbon related to **COT** *via* a transannular ring closure[23] that forces it to adopt a coplanar structure and thus yields a Hückel antiaromatic system. As a consequence **Pn** dimerises *via* a [2 + 2] cycloaddition pathway (*c.f.* cyclobutadiene) above −196 °C to form a non-aromatic pentafulvene-type system.[24,25] This process indicates the presence of a low-lying triplet state since such a reaction is believed to proceed *via* diradical intermediates.[26] The increased rigidity imparted by the transannular bond also

[a]*Department of Chemistry and Institute for Sustainability, University of Bath, Claverton Down, Bath BA2 7AY, UK. E-mail: u.hintermair@bath.ac.uk*

[b]*Julius-Maximilians-Universität Würzburg, Institute of Inorganic Chemistry and Institute for Sustainable Chemistry & Catalysis with Boron, Am Hubland, 97074 Würzburg, Germany. E-mail: holger.helten@uni-wuerzburg.de*

[c]*Chemical Characterisation Facility, University of Bath, Claverton Down, Bath BA2 7AY, UK*

† Electronic supplementary information (ESI) available: Experimental and computational details, additional analytical data (NMR, XRD). CCDC 2335451. For ESI and crystallographic data in CIF or other electronic format see DOI: https://doi.org/10.1039/d4sc06439a

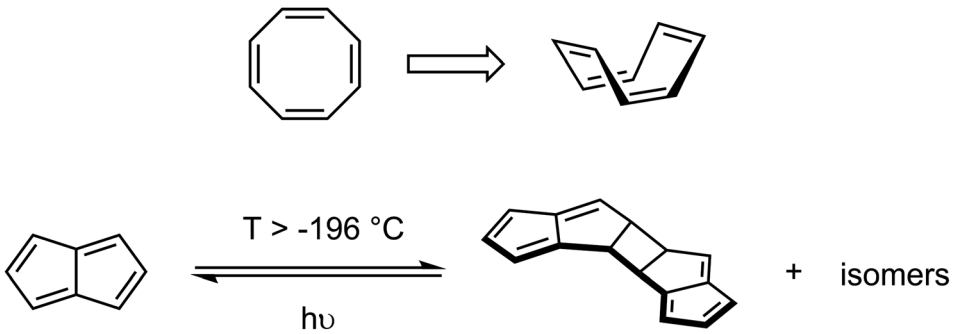

Scheme 1 Examples of carbocyclic 8π systems: non-planar conformation of **COT** (top) and dimerization of **Pn** (bottom).

prevents conformational rearrangements that are often seen when switching between aromatic and antiaromatic states of larger molecules.[27–34] However, to date no crystallographic data of a pentalene and its corresponding pentalenide have been reported to compare the extent of any changes.

The most common method to stabilise (or conceal) the antiaromatic character of pentalene is through annelation with other π systems such as in benzopentalenes, with the first dibenzopentalene reported in 1912, nearly 50 years prior to the first report of an isolable **Pn**.[35,36] Conjugation of the pentalene to locally aromatic benzene groups imparts stability onto the antiaromatic core and renders dibenzopentalenes to be bench-stable despite being formally Hückel antiaromatic $4n$ π-electron systems.[16,18,37–39] Annelation can also be used to vary the degree of (anti)aromaticity, as shown for dinaphtho[2,1,*a*,*f*]pentalene,[40] an effect which is useful for tuning the electronics of polycyclic pentalene derivatives for potential use in organic semiconductors.[41–43]

However, reports of stable **Pn** derivatives that do not rely on annelation with aromatic groups are sparse (Fig. 1).[44–50] 1,3,5-^{t}Bu$_3$Pn was the first **Pn** derivative to be characterised by single crystal XRD which confirmed the coplanarity of the two rings in the **Pn** core and showed bond alternation consistent with localised C=C bonds.[51] The stabilisation of 1,3,5-^{t}Bu$_3$Pn arises from the steric bulk of the ^{t}Bu substituents providing a high kinetic barrier that prevents the [2 + 2] cycloaddition from occurring; the less sterically hindered derivatives 1,3-^{t}Bu$_2$-5-RPn (R = CO_2Me, CHO or CN) were found to exist in equilibrium with their [2 + 2] dimers.[49] 1,2,3,4,5,6-hexamethylpentalene (**Pn***) avoids forming an antiaromatic π-system through an exocyclic C=C bond which results in the **Pn** core not being fully sp^2 hybridised.[44] The corresponding [2 + 2] dimer could be accessed through oxidation of the dianion **Pn***$^{2-}$ by $FeCl_2$.[52] Another hexasubstituted **Pn**, an amino-pentalenecarbonitrile, was reported by Hartke where the opposing push–pull effects of the amino and nitrile groups were proposed to electronically stabilise the antiaromatic core.[45] A thienylpentalene has been reported where the aromatic heterocycle stabilises the antiaromaticity of the core as in benzopentalenes. In the same report a hexaarylated **Pn** derivative bearing *p*-tolyl substituents was described.[50] The hexasubstitution pattern is likely to impart a significant steric barrier to

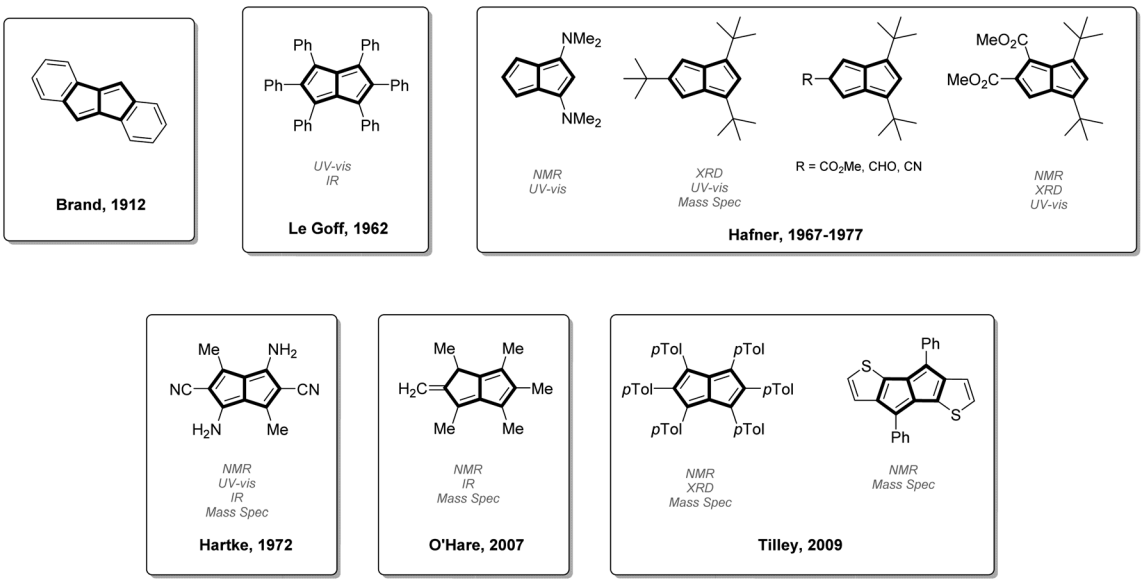

Fig. 1 Previously reported stable pentalene derivatives and their means of characterisation.

the [2 + 2] dimerisation, however, the electronic influence of the aromatic tolyl-substituents on the **Pn** core is unknown. More recently a tetra-substituted **Pn** with cyclopropyl groups was described, however, the cyclo-propyl groups did not impart enough steric or electronic stabilisation to prevent [2 + 2] dimerisation.[53] Le Goff reported the synthesis of hexaphenylpentalene from the base-catalysed condensation of a cyclopentadiene with an α,β-unsaturated carbonyl compound followed by oxidation of the resultant dihydropentalene.[36] Whilst the synthetic rationale of forming substituted $\mathbf{PnH_2}$ from cyclopentadienes and α,β-unsaturated carbonyls is a well-established pathway,[54–58] the subsequent oxidation of $\mathbf{PnH_2}$ to **Pn** is less well known. Le Goff also noted that a sample of $\mathbf{Li_2[Ph_6Pn]}$ could be oxidised by addition of I_2 to yield $\mathbf{Ph_6Pn}$,[36] a route that in theory should allow facile formation of **Pn** derivatives where the only by-product would be an inorganic salt. Recently we reported the synthesis of the first alkaline earth pentalenide $\mathbf{Mg[Ph_4Pn]}$.[59] Herein we report the remarkably facile and fully reversible oxidation of $\mathbf{Mg[Ph_4Pn]}$ to $\mathbf{Ph_4Pn}$ which has been fully characterised by NMR and UV-vis spectroscopy as well as X-ray diffraction. The antiaromaticity of the **Pn** core and the steric and electronic influence of the phenyl substituents have been investigated by computational studies.

2. Results and discussion

The addition of one equivalent of iodine to a THF solution of $\mathbf{Mg[Ph_4Pn]}$ at room temperature led to an immediate colour change from bright orange to dark yellow, with a precipitate of MgI_2 forming after a few minutes. NMR spectroscopic analysis of the filtered solution showed the complete and selective formation of $\mathbf{Ph_4Pn}$ (Fig. 2). When either an excess of iodine or an equivalent of bromine was used instead, an unidentifiable mixture of products originating from unselective (over)oxidation was observed. This difference in reactivity can be attributed to the increased oxidation power of Br_2 over I_2 ($E^0 = 1.07$ V for Br_2; $E^0 = 0.54$ V for I_2)[60] and its propensity to undergo bromination reactions. Previous attempts to oxidise $\mathbf{Ph_4PnH_2}$ or $\mathbf{Ph_4Pn^{2-}}$ to $\mathbf{Ph_4Pn}$ with *N*-bromosuccinimide were unsuccessful,[61] although Cu(II), which has a lower oxidation potential ($E^0 = 0.34$ V) than iodine, has previously been reported to facilitate the oxidative coupling of $\mathbf{Li_2[Pn]}$ to afford $\mathbf{[Pn]_2}$.[25,62]

The room temperature ^{1}H NMR spectrum of $\mathbf{Ph_4Pn}$ showed a C_{2h} symmetrical molecule with three well-resolved, diamagnetic signals observed at 7.14, 7.05 and 5.44 ppm (Fig. 2). The chemical shift of the two equivalent wingtip protons $\mathbf{H_w}$ in $\mathbf{Ph_4Pn}$ was found to be 1.5 ppm upfield relative to $\mathbf{Ph_4Pn^{2-}}$ (Table 1), and the corresponding wingtip carbons $\mathbf{C_w}$ had a resonance at 134.9 ppm, a 20 ppm downfield shift relative to the respective signal in $\mathbf{Ph_4Pn^{2-}}$. These shifts are consistent with formation of a localised olefinic π-system arising from an 8π antiaromatic pentalene and indicate full oxidation of the core of $\mathbf{Ph_4Pn^{2-}}$ to $\mathbf{Ph_4Pn}$, with the four equivalent phenyl groups remaining largely unperturbed. The cleanliness of the crude ^{1}H NMR spectrum also indicates that in solution there is no significant [2 + 2] dimer formation. Variable temperature NMR studies from −80 °C to 60 °C in THF showed no discernible changes (Fig. S4†), indicating monomeric $\mathbf{Ph_4Pn}$ to be remarkably stable under inert conditions, although exposure to air quickly led to decomposition.

XRD analysis of single crystals grown from THF at −35 °C confirmed the structure of $\mathbf{Ph_4Pn}$ with retention of a bicyclic, coplanar **Pn** core (Fig. 3). Bond alternation within the sp^2 perimeter was evident by C–C distances within the **Pn** ring ranging from 1.388(2)–1.464(3) Å. For comparison, the average C–C bond length in $\mathbf{Mg[Ph_4Pn]}$ was found to range between 1.406(3)–1.455(3) Å (Table 1).[59] The C=C bond lengths in $\mathbf{Ph_4Pn}$ were longer than in the non-aromatic $\mathbf{Ph_4PnH_2}$ (1.36(1)–1.37(1) Å)[57] in reflection of its antiaromatic character. The C–C bridgehead bond length of 1.450(3) Å was identical to the equivalent distance in $\mathbf{Mg[Ph_4Pn]}$ (1.451(3) Å), suggesting the electronics of the **Pn** core do not significantly influence this bond. The C–C/C=C bond alternation found in $\mathbf{Ph_4Pn}$ was less pronounced than in $\mathbf{1,3,5\text{-}^tBu_3Pn}$ where the C–C bonds ranged

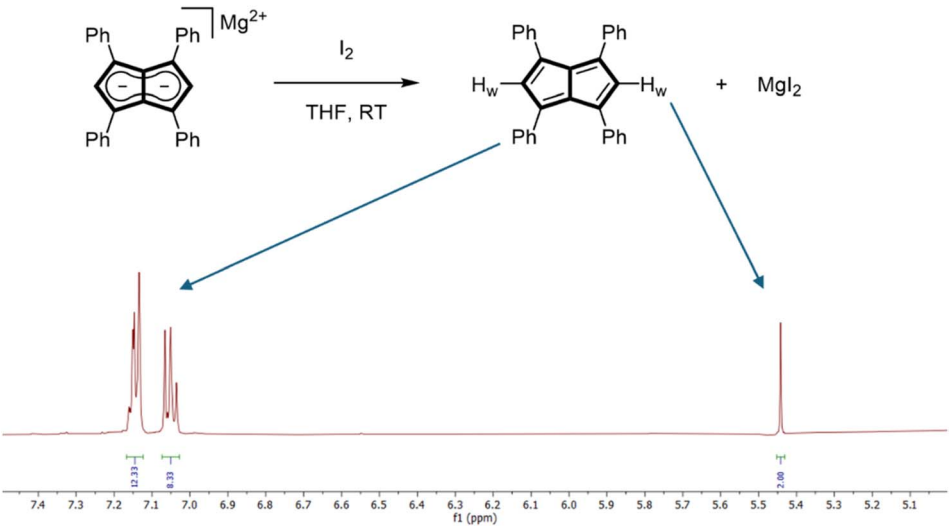

Fig. 2 Synthesis of $\mathbf{1,3,4,6\text{-}Ph_4Pn}$ (top) and its 500 MHz room temperature ^{1}H NMR spectrum in THF-H_8 (bottom).

Table 1 Key analytical features of Ph_4PnH_2, Mg[Ph_4Pn], Ph_4Pn and $[Ph_4Pn]_2$

	δ ^1H_w[a] ($^{13}C_w$)/ppm	C–C perimeter/Å	C–C bridge/Å	Aryl twist angle/°
Ph_4PnH_2	7.45 (139.4)	1.357(6)–1.512(8)	1.448(7)	43.3–47.0
Mg[Ph_4Pn]	6.80 (115.5)	1.406(3)–1.455(3)	1.451(3)	17.1–35.2
Ph_4Pn	5.42 (134.9)	1.388(2)–1.464(3)	1.450(3)	31.7–42.3
$[Ph_4Pn]_2$	n/a	1.357(2)–1.517(2)	1.471(2), 1.476(2)	11.9–47.3

[a] Data for Ph_4PnH_2 in acetone-d_6, **Mg[Ph_4Pn]** and **Ph_4Pn** in THF-H_8.

from 1.46–1.54 Å and the C=C bonds between 1.28–1.41 Å, which is likely a consequence of the different electronic nature of the substituents on the pentalene core (alkyl *versus* aryl).[51] No stacking of **Ph_4Pn** was observed in the solid or solution state, ruling out the formation of a so-called "3D aromatic" system as a means of alleviating the antiaromatic 8π count.[64–66]

As in **Mg[Ph_4Pn]** and **Ph_4PnH_2**, the phenyl substituents in **Ph_4Pn** were twisted *versus* the plane of the **Pn** core by 31.7(3)–42.3(3) Å.[57,59] This value was larger than in **Mg[Ph_4Pn]** but marginally less than the non-aromatic **Ph_4PnH_2** (Table 1). In **Mg[Ph_4Pn]** the phenyl groups strive to adopt a co-planar arrangement to delocalise the negative charge as much as sterically possible,[67] whilst in **Ph_4Pn** and **Ph_4PnH_2** there is no charge to distribute and so the phenyl groups likely relax in a slightly larger twist angle to minimise steric clash.

Serendipitously, the [2 + 2] cycloaddition dimer **$[Ph_4Pn]_2$** was found to co-crystallise with **Ph_4Pn** in the same unit cell. In this structure two **Pn** units were connected *via* a cyclobutane bridge in an extended chair-like conformation (Fig. 4). The [2 + 2] cycloaddition means that **$[Ph_4Pn]_2$** is formally non-aromatic with each 6π pentafulvene units containing two adjacent sp^3 centres. The C=C bond lengths in **$[Ph_4Pn]_2$** ranged between 1.357(2)–1.374(2) Å and are contracted relative to the antiaromatic **Ph_4Pn** (Table 1), more reminiscent of those found for the non-aromatic **Ph_4PnH_2** which **$[Ph_4Pn]_2$** is most closely related to.[57] The sp^3 bonds within the cyclobutane unit were significantly longer than the other sp^2 bonds in the dimer, with bond lengths of 1.567(2)–1.675(2) Å. Sun and co-workers reported similar, but marginally shorter, bond lengths of the cyclobutane linkage (1.56–1.60 Å) for their **$[^cPr_4Pn]_2$**.[53] O'Hare and co-workers reported that reaction of ***cis*-$(Me_3Sn)_2$Pn*** with $FeCl_2$ resulted in oxidation of the pentalenide followed by dimerisation, however, no crystallographic data are available for **[Pn*]$_2$**.[52]

Geometry optimisation of **Ph_4Pn** at the B3LYP/6-311++g(d,p) level of theory in the gas phase gave good agreement with the crystallographic data, including the 39.2–44.5° twist angle of the phenyl groups. This suggests the origin of the rotation not to be due to packing effects in the solid state, but to arise so as to avoid overlap of the aromatic (phenyl groups) and antiaromatic (pentalene core) ring currents. The calculated C–C perimeter range of 1.37–1.48 Å for the pentalene core and 1.45 Å for the C–C bridge also matched well with the crystallographic data.

To investigate the extent of antiaromaticity in **Ph_4Pn**, harmonic oscillator model of aromaticity (HOMA) calculations were performed using the experimental X-ray data, alongside DFT calculations of the anisotropy of the induced current density (ACID) and calculations on the nucleus independent

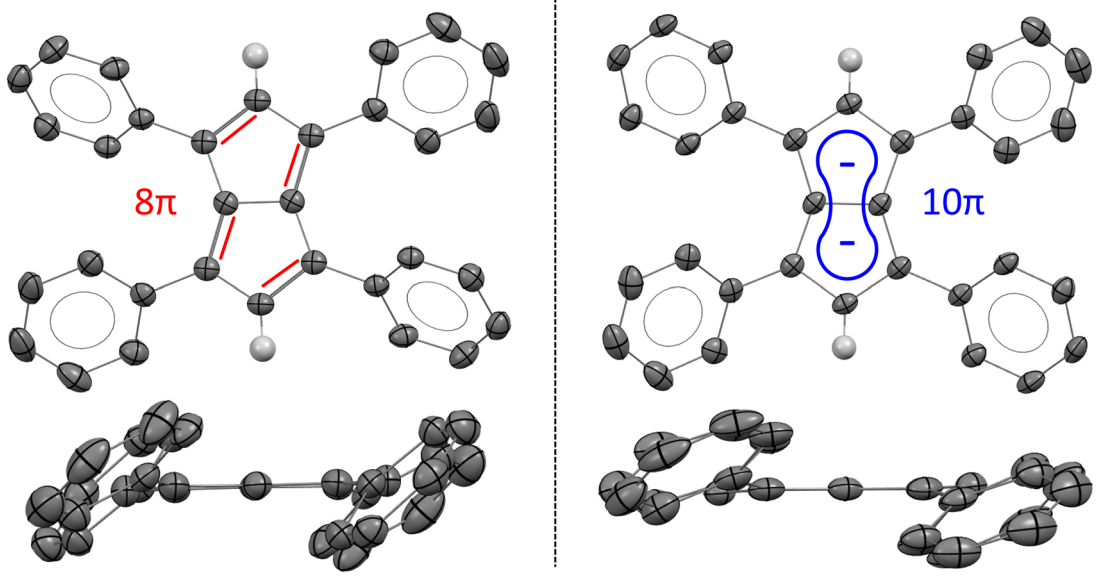

Fig. 3 X-ray crystal structures of **1,3,4,6-Ph_4Pn** (left; top and side views) and **1,3,4,6-Ph_4Pn^{2-}** (right; top and side views)[63] with thermal ellipsoids at the 50% probability level. Phenyl hydrogen atoms omitted for clarity, and double bonds and aromatic conjugation added for illustration.

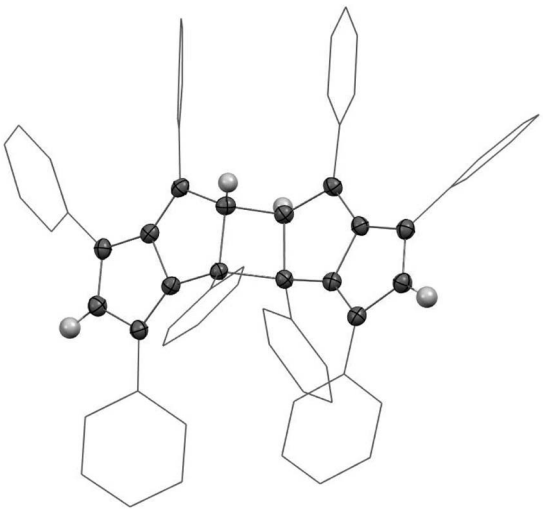

Fig. 4 X-ray crystal structure of [1,3,4,6-Ph_4Pn]$_2$ with thermal ellipsoids at the 50% probability level (phenyl hydrogen atoms omitted for clarity).

chemical shift (NICS) along different axes of the molecule (Fig. 5). A $HOMA_B$ value of 0.28 was found for the pentalene core, with the phenyl groups returning a value of 0.99 indicating no overlap of the two π-systems. The lack of overlap is also reflected in the NICS scan along the *Z*-axis through the centre of one phenyl group. This returned a value for the out-of-plane component of the chemical shift of −26.34 ppm at $Z = 0.7$ Å, which is very close to that of unsubstituted benzene (Fig. S6†).[68] In contrast to the dianionic tetraphenylpentalenide,[67] the ESP map of neutral **Ph_4Pn** showed an equally distributed charge density over the pentalene core and the flanking phenyl groups (Fig. S10†). The aromatic pentalenide core of **Ph_4Pn^{2-}** gave a $HOMA_B$ value of 0.63, showing a clear change in aromaticity between the 8π and 10π versions of the molecule. The ACID plot of **Ph_4Pn** showed a strong paratropic ring current about the perimeter of the pentalene core with a significant contribution from the transannular C–C bridge. The diatropic ring currents of the four aromatic phenyl substituents were clearly separated and essentially unperturbed by the presence of the antiaromatic core, as indicated by the corresponding $HOMA_B$ values. The NICS scan along the *Z*-axis, starting from the centre of one 5-membered ring running perpendicular to the pentalene plane, showed features characteristic of an antiaromatic π system (Fig. 5). The isotropic shift values were positive throughout the scan, with a maximum of 24.15 ppm at $Z = 0.4$ Å, and the shape of the curve was strongly dominated by the out-of-plane component of the chemical shift. The NICS-*Y* scan,

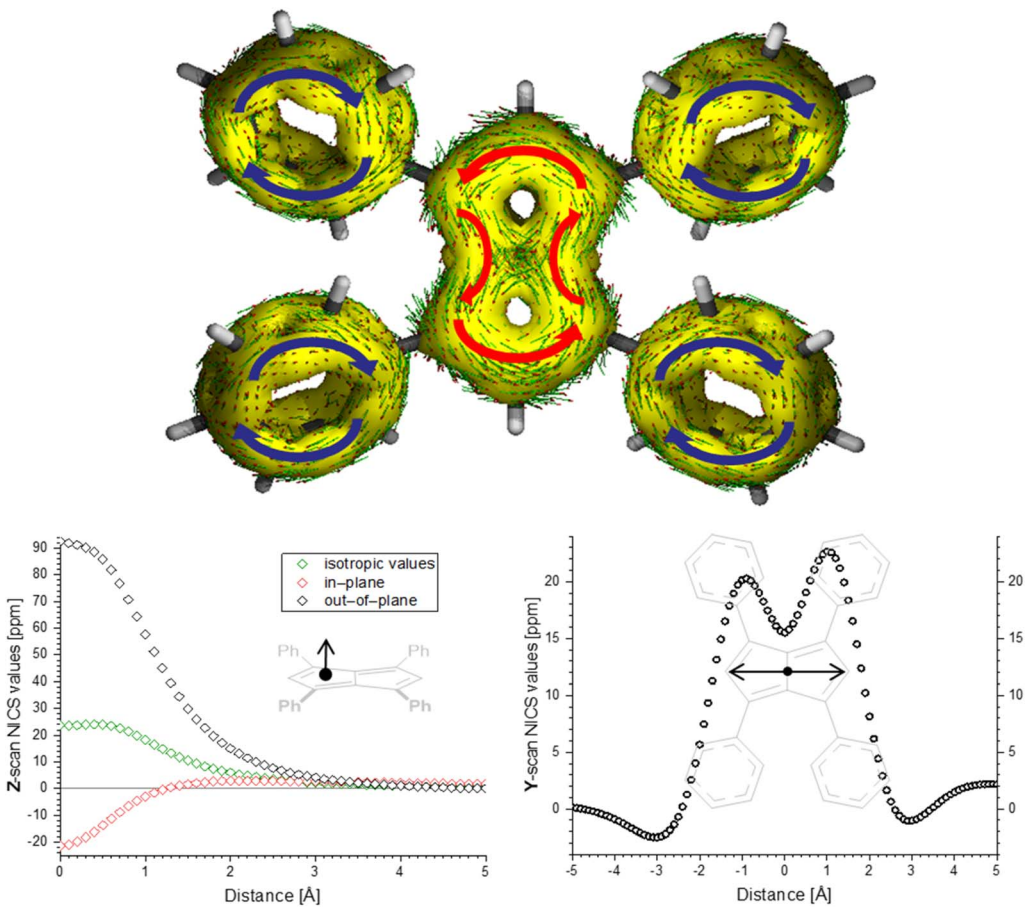

Fig. 5 ACID plot ((top); iso-value = 0.03) and NICS scans ((bottom); *Z* scan [left] and *Y* scan [right], at a *Z* height of 1.7 Å; NICS probe BQ shown as •) of Ph_4Pn.

running parallel to the pentalene plane at a height of 1.7 Å revealed two maxima at $Y = -0.9$ Å (20.28 ppm) and at $Y = 1$ Å (22.67 ppm) close to the centres of each 5-membered ring, consistent with the paratropic current found in the ACID plot, and mirrors that of the strongly aromatic dianion **Ph_4Pn^{2-}**.[67] These maxima were separated by a local minimum at the centre of the molecule around the transannular C–C bridge ($Y = 0$ Å, 15.50 ppm) as a result of two contributions: a paratropic current about the perimeter of the pentalene system combined with two local paratropic currents in each 5-membered ring. As observed by Stanger *et al.* for unsubstituted pentalene, the latter contribution typically dominates in these systems,[69] although retaining some global antiaromaticity. This strong influence of local currents in the two 5-membered rings can also be seen by the turbulence around the transannular C–C bridge in the ACID plot of **Ph_4Pn** (Fig. 5). The NICS and ACID calculations for the [2 + 2] cycloaddition product **$[Ph_4Pn]_2$** showed a complete loss of the antiaromatic current (Fig. S12;† with only the flanking phenyl rings retaining their aromatic character), consistent with the notion that the dimerisation of pentalenes is driven by a relief of antiaromatic destabilisation.

The computed frontier orbitals of **Ph_4Pn** (Fig. 6) agree well with those calculated for unsubstituted **Pn**.[70] Both the HOMO and the LUMO are characterised as π orbitals of the pentalene system, with minimal contribution from the substituents. The

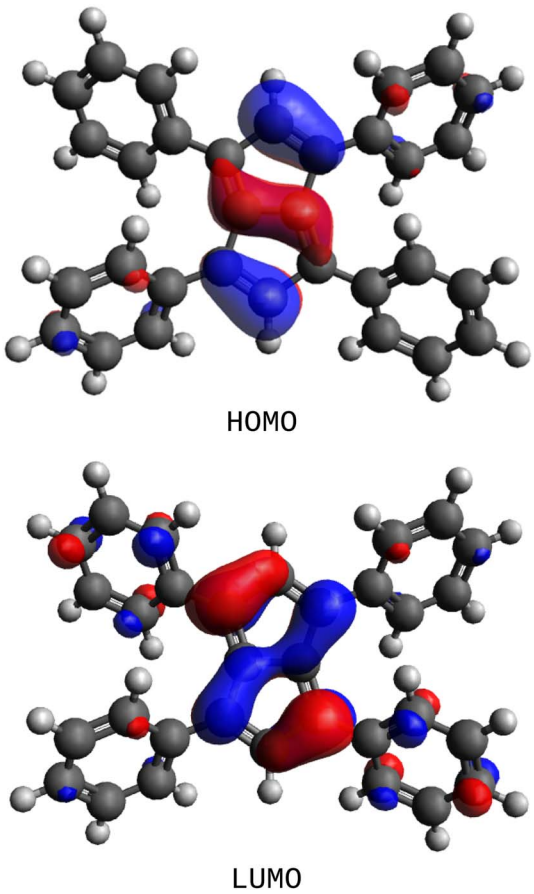

Fig. 6 Frontier molecular orbitals of Ph_4Pn.

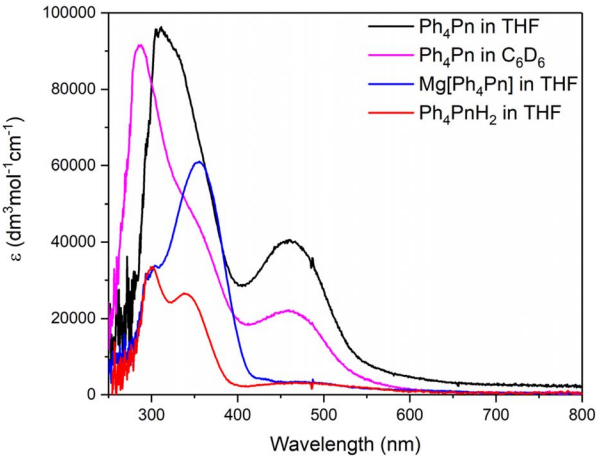

Fig. 7 UV-vis spectra of **1,3,4,6-Ph_4Pn** (6 μM), **Mg[Ph_4Pn]** (15 μM) and Ph_4PnH_2 (11 μM) in THF at 298 K.

HOMO showed major contributions from the localised trisubstituted C=C bond in each C_5-ring, polarised towards the wingtip carbon, as well as a noticeable contribution from the transannular C–C bond. In contrast, in the HOMO of **Ph_4Pn^{2-}** the largest contributions were found to be localised on the 1,3,4,6-positions.[67] The LUMO of **Ph_4Pn** showed increased delocalisation across the transannular bond into the 1,4-*ipso*-carbons but (unlike in **Ph_4Pn^{2-}**) without any delocalisation into the phenyl substituents. The HOMO–LUMO gap for **Ph_4Pn** of 2.11 eV was about 1 eV smaller than that of **Ph_4Pn^{2-}** (3.15 eV), indicating a more reactive system due to the antiaromatic core. **Pn** has been calculated to have a HOMO–LUMO gap of 1.12 eV,[70] 1 eV smaller than for **Ph_4Pn** emphasising the stabilising influence of the four phenyl substituents. A singlet-triplet gap of 41.1 kJ mol^{-1} (0.43 eV) was calculated for **Ph_4Pn**, about four times greater than that computed for **Pn** (0.1 eV),[71] highlighting the decreased propensity of **Ph_4Pn** to dimerise through increased kinetic stabilisation of the singlet state.

The UV-vis spectrum of **Ph_4Pn** in THF gave rise to two broad absorptions (Fig. 7). The first band at $\lambda_{max} = 312$ nm ($\varepsilon = 95\,000$ M^{-1} cm^{-1}) was nearly three times more intense than comparable absorptions observed for **Ph_4PnH_2** ($\lambda = 301$, $\varepsilon = 31\,500$ M^{-1} cm^{-1} and $\lambda = 339$ nm, $\varepsilon = 26\,800$ M^{-1} cm^{-1}) and are attributed to electronic transitions from the HOMO−1 into the LUMO+2 and LUMO+3 on the basis of TD-DFT (Fig. S16†). The second maximum at $\lambda_{max} = 460$ nm ($\varepsilon = 40\,000$ M^{-1} cm^{-1}) is assigned as a HOMO−1 → LUMO transition. A similar absorption was seen for **Ph_4PnH_2** at 468 nm, though an order of magnitude less intense ($\varepsilon = 3600$ M^{-1} cm^{-1}), and was assigned to the fulvene-like double bond in the molecule.[57] The UV-vis spectrum of **Ph_4Pn** in benzene largely retained the same features as in THF, indicating there is no significant change in the solution structure of **Ph_4Pn** between the two solvents, consistent with the NMR data. The main band at $\lambda_{max} = 275$ nm was of slightly lower intensity ($\varepsilon = 90\,000$ M^{-1} cm^{-1}) and blue shifted by 50 nm compared to the same absorption in THF. A marginally more pronounced shoulder at $\lambda_{max} = 350$ nm was seen in the benzene spectrum and accounted for by TD-DFT

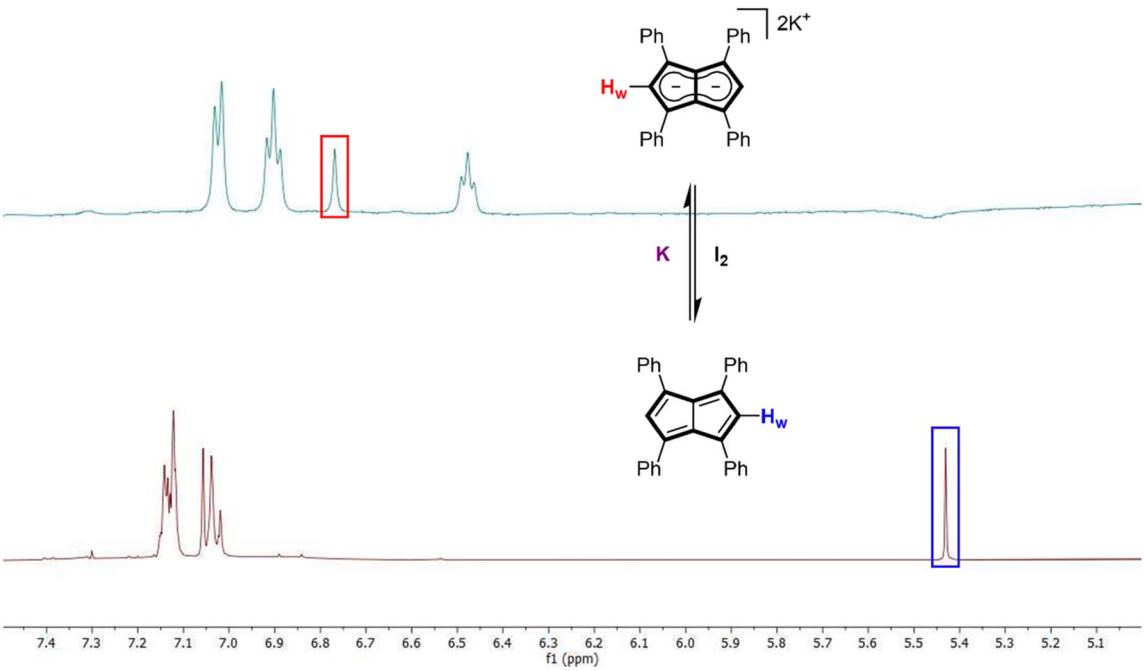

Fig. 8 500 MHz ^{1}H NMR spectra of $K_2[Ph_4Pn]$ (top) and 1,3,4,6-Ph_4Pn (bottom).

(Fig. S16†). Dilute solutions of **Ph_4Pn** in THF and benzene were both pale yellow due to the absorption at 460 nm, even though in benzene this band was only about half the intensity than in THF. **1,3,5-^{t}Bu$_3$Pn** has been reported to be dark blue in colour with a visible absorption at 598 nm, and **1,3-$(NMe_2)_2$Pn**, **1,4-Me_2-2,5-$(CN)_2$-3,6-$(NH_2)_2$Pn** and **Ph_6Pn** were also reported to have absorptions >600 nm. Similar low energy absorptions were found computationally for **Ph_4Pn** but with much lower intensities (Fig. S16 and S17†).

In line with the electrochemistry of **Ph_4Pn** showing a reduction peak ∼0.3 V *vs.* NHE in THF (Fig. S18†), **Ph_4Pn** can be reduced back to **Ph_4Pn^{2-}** by contacting a THF solution of **Ph_4Pn** with a freshly prepared potassium mirror, causing an immediate colour change from dark yellow to bright red. The ^{1}H NMR spectrum of the solution showed full consumption of **Ph_4Pn** and the spectroscopically quantitative formation of **$K_2[Ph_4Pn]$** (Fig. 8) with a characteristic **H_w** shift of 6.76 ppm.[57] The ease of the reduction back to the aromatic **Ph_4Pn^{2-}** is supported by DFT where the enthalpy of **Ph_4Pn** was found to be 72.8 kJ mol^{-1} higher than **Ph_4Pn^{2-}**.

3. Conclusion

A stable pentalene has been synthesised through the facile oxidation of its corresponding pentalenide using elemental iodine. Unlike previous reports of pentalenes, **Ph_4Pn** crystallised as a mixture of both the monomer and dimer in the same unit cell. However, NMR spectroscopy showed that in solution the monomeric form dominates, and UV-vis spectroscopy indicated no solvatochromism or change in the solution structure in THF and benzene. **Ph_4Pn** is a rare example of a small molecule featuring both Hückel aromatic and anti-aromatic subunits in close proximity, albeit electronically separated from each other as shown by quantum chemical calculations. Therefore, the stabilisation of the anti-aromatic pentalene core imparted by the four aromatic phenyl substituents is largely steric in nature. The reduction of **Ph_4Pn** back to **Ph_4Pn^{2-}** was found to be reversible within a potential range of ∼1 V, representing a unique example of a small hydrocarbon that can easily switch between an aromatic and anti-aromatic state without any conformational or skeletal rearrangements. These properties alongside its structural simplicity and ease of synthesis[58,67] suggest that **Ph_4Pn** and its derivatives could find applications similar to those of dibenzopentalenes in electrochemical sensing or optoelectronics. In the context of organometallic chemistry, the facile oxidation of **Ph_4Pn^{2-}** by iodine provides a useful threshold for the redox potential of metal ions bound to it to guide the design and synthesis of novel pentalenide complexes.

Data availability

Crystallographic datasets are available from the CCDC deposition number 2335451, and other analytical data can be found in the ESI.†

Author contributions

HJS carried out all synthetic work, spectroscopic analyses, electrochemistry, and drafted the manuscript. GKK conducted all XRD analyses. AH carried out all calculations with guidance and supervision by HH. UH led the project, and all authors contributed to refining the manuscript.

Conflicts of interest

The authors declare no conflicts of interest.

Acknowledgements

UH and HJS thank the Royal Society (award UF160458) and the University of Bath for funding this work. HH and AH thank the German Research Foundation (DFG) for funding through the Heisenberg Grant HE 6171/9-1 (468457264). Kathryn Proctor (University of Bath) is acknowledged for assistance with conducting the mass spectrometry measurements, and we thank Simon Lewis and Dan Pantos (University of Bath) for stimulating discussions about aromaticity.

References

1 M. Solà, Aromaticity Rules, *Nat. Chem.*, 2022, **14**(6), 585–590, DOI: 10.1038/s41557-022-00961-w.
2 W. E. von Doering and F. L. Detert, Cycloheptatrienylium Oxide, *J. Am. Chem. Soc.*, 1951, **73**(2), 876–877, DOI: 10.1021/JA01146A537.
3 E. Hückel, Quantentheoretische Beiträge Zum Benzolproblem - I. Die Elektronenkonfiguration Des Benzols Und Verwandter Verbindungen, *Z. Phys.*, 1931, **70**(3–4), 204–286, DOI: 10.1007/BF01339530.
4 R. Breslow, Antiaromaticity, *Acc. Chem. Res.*, 1973, **6**(12), 393–398, DOI: 10.1021/AR50072A001.
5 G. Merino, M. Solà, I. Fernández, C. Foroutan-Nejad, P. Lazzeretti, G. Frenking, H. L. Anderson, D. Sundholm, F. P. Cossío, M. A. Petrukhina, J. Wu, J. I. Wu and A. Restrepo, Aromaticity: Quo Vadis, *Chem. Sci.*, 2023, **14**(21), 5569–5576, DOI: 10.1039/D2SC04998H.
6 P. Lazzeretti, Ring Currents, *Prog. Nucl. Magn. Reson. Spectrosc.*, 2000, **36**(1), 1–88, DOI: 10.1016/S0079-6565(99)00021-7.
7 N. C. Baird, Quantum Organic Photochemistry. II. Resonance and Aromaticity in the Lowest 3ππ* State of Cyclic Hydrocarbons, *J. Am. Chem. Soc.*, 1972, **94**(14), 4941–4948, DOI: 10.1021/JA00769A025.
8 H. Ottosson, Exciting Excited-State Aromaticity, *Nat. Chem.*, 2012, **4**(12), 969–971, DOI: 10.1038/nchem.1518.
9 C. S. Wannere, C. Corminboeuf, Z. X. Wang, M. D. Wodrich, R. B. King and P. V. R. Schleyer, Evidence for d Orbital Aromaticity in Square Planar Coinage Metal Clusters, *J. Am. Chem. Soc.*, 2005, **127**(15), 5701–5705, DOI: 10.1021/JA042716Q.
10 A. C. Tsipis, C. E. Kefalidis and C. A. Tsipis, The Role of the 5f Orbitals in Bonding, Aromaticity, and Reactivity of Planar Isocyclic and Heterocyclic Uranium Clusters, *J. Am. Chem. Soc.*, 2008, **130**(28), 9144–9155, DOI: 10.1021/JA802344Z.
11 I. A. Popov, A. A. Starikova, D. V. Steglenko and A. I. Boldyrev, Usefulness of the σ-Aromaticity and σ-Antiaromaticity Concepts for Clusters and Solid-State Compounds, *Chem.–Eur. J.*, 2018, **24**(2), 292–305, DOI: 10.1002/CHEM.201702035.
12 J. T. Boronski, J. A. Seed, D. Hunger, A. W. Woodward, J. van Slageren, A. J. Wooles, L. S. Natrajan, N. Kaltsoyannis and S. T. Liddle, A Crystalline Tri-Thorium Cluster with σ-Aromatic Metal–Metal Bonding, *Nature*, 2021, **598**(7879), 72–75, DOI: 10.1038/s41586-021-03888-3.
13 B. Peerless, A. Schmidt, Y. J. Franzke and S. Dehnen, φ-Aromaticity in Prismatic {Bi_6}-Based Clusters, *Nat. Chem.*, 2022, **15**(3), 347–356, DOI: 10.1038/s41557-022-01099-5.
14 A. Minsky, A. Y. Meyer and M. Rabinovitz, Paratropicity and Antiaromaticity: Role of the Homo-Lumo Energy Gap, *Tetrahedron*, 1985, **41**(4), 785–791, DOI: 10.1016/S0040-4020(01)96458-0.
15 C. Gellini and P. R. Salvi, Structures of Annulenes and Model Annulene Systems in the Ground and Lowest Excited States, *Symmetry*, 2010, **2**(4), 1846–1924, DOI: 10.3390/SYM2041846.
16 J. Sprachmann, T. Wachsmuth, M. Bhosale, D. Burmeister, G. J. Smales, M. Schmidt, Z. Kochovski, N. Grabicki, R. Wessling, E. J. W. List-Kratochvil, B. Esser and O. Dumele, Antiaromatic Covalent Organic Frameworks Based on Dibenzopentalenes, *J. Am. Chem. Soc.*, 2023, **145**, 2840–2851, DOI: 10.1021/JACS.2C10501.
17 D. T. Chase, A. G. Fix, S. J. Kang, B. D. Rose, C. D. Weber, Y. Zhong, L. N. Zakharov, M. C. Lonergan, C. Nuckolls and M. M. Haley, 6,12-Diarylindeno[1,2-b]Fluorenes: Syntheses, Photophysics, and Ambipolar OFETs, *J. Am. Chem. Soc.*, 2012, **134**(25), 10349–10352, DOI: 10.1021/JA303402P.
18 H. Hopf, Pentalenes—From Highly Reactive Antiaromatics to Substrates for Material Science, *Angew. Chem., Int. Ed.*, 2013, **52**(47), 12224–12226, DOI: 10.1002/ANIE.201307162.
19 Z. Zeng, X. Shi, C. Chi, J. T. López Navarrete, J. Casado and J. Wu, Pro-Aromatic and Anti-Aromatic π-Conjugated Molecules: An Irresistible Wish to Be Diradicals, *Chem. Soc. Rev.*, 2015, **44**(18), 6578–6596, DOI: 10.1039/C5CS00051C.
20 G. E. Rudebusch, J. L. Zafra, K. Jorner, K. Fukuda, J. L. Marshall, I. Arrechea-Marcos, G. L. Espejo, R. Ponce Ortiz, C. J. Gómez-García, L. N. Zakharov, M. Nakano, H. Ottosson, J. Casado and M. M. Haley, Diindeno-Fusion of an Anthracene as a Design Strategy for Stable Organic Biradicals, *Nat. Chem.*, 2016, **8**(8), 753–759, DOI: 10.1038/nchem.2518.
21 L. J. Karas and J. I.-C. Wu, Antiaromatic Compounds: A Brief History, Applications, and the Many Ways They Escape Antiaromaticity, in *Aromaticity: Modern Computational Methods and Applications*, ed. I. Fernandez, Elsevier, 2021, pp 319–338, DOI: 10.1016/B978-0-12-822723-7.00010-8.
22 F. Glöcklhofer, Concealed Antiaromaticity, *ChemRxiv*, 2023, DOI: 10.26434/CHEMRXIV-2023-HNL0W-V2.
23 S. A. R. Knox, F. Gordon and A. Stone, Approaches to the Synthesis of Pentalene *via* Metal Complexes, *Acc. Chem. Res.*, 1974, **7**(10), 321–328.
24 R. Bloch, R. A. Marty and P. de Mayo, 1-Methylpentalene, *J. Am. Chem. Soc.*, 1971, **93**(12), 3071–3072, DOI: 10.1021/ja00741a056.
25 T. Bally, S. Chai, M. Neuenschwander and Z. Zhu, Pentalene: Formation, Electronic, and Vibrational Structure, *J. Am. Chem. Soc.*, 1997, **119**(8), 1869–1875, DOI: 10.1021/ja963439t.

26 S. Poplata, A. Tröster, Y. Q. Zou and T. Bach, Recent Advances in the Synthesis of Cyclobutanes by Olefin [2+2] Photocycloaddition Reactions, *Chem. Rev.*, 2016, **116**(17), 9748–9815, DOI: 10.1021/ACS.CHEMREV.5B00723.

27 W. Stawski, Y. Zhu, Z. Wei, M. A. Petrukhina and H. L. Anderson, Crystallographic Evidence for Global Aromaticity in the Di-Anion and Tetra-Anion of a Cyclophane Hydrocarbon, *Chem. Sci.*, 2023, **14**(48), 14109–14114, DOI: 10.1039/D3SC04251K.

28 W. Stawski, Y. Zhu, I. Rončević, Z. Wei, M. A. Petrukhina and H. L. Anderson, The Anti-Aromatic Dianion and Aromatic Tetraanion of [18]Annulene, *Nat. Chem.*, 2024, 1–5, DOI: 10.1038/s41557-024-01469-1.

29 T. Y. Gopalakrishna and V. G. Anand, Reversible Redox Reaction Between Antiaromatic and Aromatic States of 32π-Expanded Isophlorins, *Angew. Chem., Int. Ed.*, 2014, **53**(26), 6678–6682, DOI: 10.1002/ANIE.201403372.

30 S. Eder, D. J. Yoo, W. Nogala, M. Pletzer, A. Santana Bonilla, A. J. P. White, K. E. Jelfs, M. Heeney, J. W. Choi and F. Glöcklhofer, Switching between Local and Global Aromaticity in a Conjugated Macrocycle for High-Performance Organic Sodium-Ion Battery Anodes, *Angew. Chem., Int. Ed.*, 2020, **59**(31), 12958–12964, DOI: 10.1002/ANIE.202003386.

31 W. Y. Cha, T. Soya, T. Tanaka, H. Mori, Y. Hong, S. Lee, K. H. Park, A. Osuka and D. Kim, Multifaceted [36]Octaphyrin(1.1.1.1.1.1.1.1): Deprotonation-Induced Switching among Nonaromatic, Möbius Aromatic, and Hückel Antiaromatic Species, *Chem. Commun.*, 2016, **52**(36), 6076–6078, DOI: 10.1039/C6CC02051H.

32 T. Y. Gopalakrishna, J. S. Reddy and V. G. Anand, An Amphoteric Switch to Aromatic and Antiaromatic States of a Neutral Air-Stable 25π Radical, *Angew. Chem., Int. Ed.*, 2014, **53**(41), 10984–10987, DOI: 10.1002/ANIE.201406893.

33 Y. Zhu, Z. Zhou, Z. Wei, A. Tsybizova, R. Gershoni-Poranne and M. A. Petrukhina, What a Difference an Electron Makes: Structural Response of Saddle-Shaped Tetraphenylene to One and Two Electron Uptake, *ChemRxiv*, 2024, **2**(5), e202400055, DOI: 10.1002/CEUR.202400055.

34 X. Yin, Y. Zang, L. Zhu, J. Z. Low, Z. F. Liu, J. Cui, J. B. Neaton, L. Venkataraman and L. M. Campos, A Reversible Single-Molecule Switch Based on Activated Antiaromaticity, *Sci. Adv.*, 2017, **3**(10), DOI: 10.1126/SCIADV.AAO2615.

35 K. Brand, Über Gefärbte Kohlenwasserstoffe Der Diphensuccinden-Reihe. I, *Ber. Dtsch. Chem. Ges.*, 1912, **45**(3), 3071–3077, DOI: 10.1002/CBER.19120450334.

36 E. L. Goff, The Synthesis of Hexaphenylpentalene, *J. Am. Chem. Soc.*, 1962, **84**(20), 3975–3976, DOI: 10.1021/ja00879a044.

37 M. Saito, M. Nakamura and T. Tajima, New Reactions of a Dibenzo[a,e]Pentalene, *Chem.–Eur. J.*, 2008, **14**(20), 6062–6068, DOI: 10.1002/CHEM.200800451.

38 A. Konishi, Y. Okada, M. Nakano, K. Sugisaki, K. Sato, T. Takui and M. Yasuda, Synthesis and Characterization of Dibenzo[a,f]Pentalene: Harmonization of the Antiaromatic and Singlet Biradical Character, *J. Am. Chem. Soc.*, 2017, **139**(43), 15284–15287, DOI: 10.1021/JACS.7B05709.

39 P. J. Mayer, O. El Bakouri, T. Holczbauer, G. F. Samu, C. Janáky, H. Ottosson and G. London, Structure-Property Relationships in Unsymmetric Bis(Antiaromatics): Who Wins the Battle between Pentalene and Benzocyclobutadiene?, *J. Org. Chem.*, 2020, **85**(8), 5158–5172, DOI: 10.1021/ACS.JOC.9B03119.

40 A. Konishi, Y. Okada, R. Kishi, M. Nakano and M. Yasuda, Enhancement of Antiaromatic Character *via* Additional Benzoannulation into Dibenzo[a,f]Pentalene: Syntheses and Properties of Benzo[a]Naphtho[2,1-f]Pentalene and Dinaphtho[2,1-a,f]Pentalene, *J. Am. Chem. Soc.*, 2019, **141**(1), 560–571, DOI: 10.1021/JACS.8B11530.

41 C. K. Frederickson, L. N. Zakharov and M. M. Haley, Modulating Paratropicity Strength in Diareno-Fused Antiaromatics, *J. Am. Chem. Soc.*, 2016, **138**(51), 16827–16838, DOI: 10.1021/JACS.6B11397.

42 S. Jalife, A. Tsybizova, R. Gershoni-Poranne and J. I. Wu, Modulating Paratropicity in Heteroarene-Fused Expanded Pentalenes, *Org. Lett.*, 2024, **26**(6), 1293–1298, DOI: 10.1021/ACS.ORGLETT.4C00188.

43 H. Oshima, A. Fukazawa and S. Yamaguchi, Facile Synthesis of Polycyclic Pentalenes with Enhanced Hückel Antiaromaticity, *Angew. Chem., Int. Ed.*, 2017, **56**(12), 3270–3274, DOI: 10.1002/ANIE.201611344.

44 A. E. Ashley, A. R. Cowley and D. O'Hare, Permethylpentalene Chemistry, *Eur. J. Org. Chem.*, 2007, **14**, 2239–2242, DOI: 10.1002/ejoc.200700033.

45 K. Hartke and R. Matusch, Aminopentalenecarbonitriles, a Group of Stable Pentalenes, *Angew. Chem., Int. Ed. Engl.*, 1972, **11**(1), 50–51, DOI: 10.1002/anie.197200501.

46 K. Hafner, K. F. Bangert and V. Orfanos, 1,3-Bis(Dimethylamino)Pentalene, *Angew. Chem., Int. Ed. Engl.*, 1967, **475**(5), 451–452.

47 K. Hafner and H. U. Süss, 1,3,5-Tri-tert-Butylpentalene. A Stabilized Planar 8π-Electron System, *Angew. Chem., Int. Ed. Engl.*, 1973, **12**(7), 575–577, DOI: 10.1002/anie.197305751.

48 K. Hafner and M. Suda, [6+2] Cycloadditions of Pentafulvene. A Facile Pentalene Synthesis, *Angew. Chem., Int. Ed. Engl.*, 1976, **15**(5), 314–315.

49 M. Suda and K. Hafner, Synthesis of 4.6-Di-Tert.-Butyl-Pentalene Derivatives and Their Reversible Dimerization, *Tetrahedron Lett.*, 1977, **18**(28), 2449–2452, DOI: 10.1016/S0040-4039(01)83790-4.

50 Z. U. Levi and T. D. Tilley, Versatile Synthesis of Pentalene Derivatives *via* the Pd-Catalyzed Homocoupling of Haloenynes, *J. Am. Chem. Soc.*, 2009, **131**(8), 2796–2797, DOI: 10.1021/JA809930F.

51 B. Kitschke and H. J. Lindner, The Crystal and Molecular Structures of Two Substituted Pentalenes, *Tetrahedron Lett.*, 1977, **18**(29), 2511–2514, DOI: 10.1016/S0040-4039(01)83806-5.

52 A. E. Ashley, R. T. Cooper, G. G. Wildgoose, J. C. Green and D. O'Hare, Homoleptic Permethylpentalene Complexes: "Double Metallocenes" of the First-Row Transition Metals,

J. Am. Chem. Soc., 2008, **130**, 15662–15677, DOI: 10.1021/ja8057138.

53 H. Zhao, R. K. Gupta, W. Zhang, J. Jia, Q. Yu, Z. Gao, G. Zhuang, D. Li, X. Wang, C. H. Tung and D. Sun, Facile One-Pot Synthesis of a Novel All-Carbon Stair Containing Dimerized Pentalene Core from Alkyne, *Chin. Chem. Lett.*, 2022, **33**(4), 2047–2051, DOI: 10.1016/J.CCLET.2021.10.036.

54 A. G. Griesbeck, Pyrrolidine-Catalyzed Reactions between α,β-Unsaturated Carbonyl Compounds and Cyclopentadiene: A Convenient Approach to 1,2-and 1,5-Dihydropentalenes, *J. Org. Chem.*, 1989, **54**(2), 4981–4982.

55 A. G. Griesbeck, Ein Effizienter Zugang Zu 1,5-Dihydropentalen Und 2-Methyl-1,5-Dihydropentalen Aus Acrolein Und Methacrolein, *Synthesis*, 1990, **2**, 144–147.

56 A. G. Griesbeck, Notizen/Notes: Synthesis of 1-Phenyl,1,2- and 4-Phenyl-1,5-Dihydropentalenes, *Chem. Ber.*, 1991, **124**(2), 403–405.

57 S. M. Boyt, N. A. Jenek, H. J. Sanderson, G. Kociok-Köhn and U. Hintermair, Synthesis of a Tetraphenyl-Substituted Dihydropentalene and Its Alkali Metal Hydropentalenide and Pentalenide Complexes, *Organometallics*, 2022, **41**(3), 211–225, DOI: 10.1021/acs.organomet.1c00495.

58 N. A. Jenek, M. Balschun, S. M. Boyt and U. Hintermair, Connect Four: Tetraarylated Dihydropentalenes and Triarylated Monocyclic Pentafulvenes from Cyclopentadienes and Enones, *J. Org. Chem.*, 2022, **87**(21), 13790–13802, DOI: 10.1021/ACS.JOC.2C01507.

59 H. J. Sanderson, G. Kociok-Köhn and U. Hintermair, Synthesis, Structure, and Reactivity of Magnesium Pentalenides, *Inorg. Chem.*, 2023, **62**(39), 15983–15991, DOI: 10.1021/ACS.INORGCHEM.3C02087.

60 *Handbook of Chemistry and Physics*, ed. J. R. Rumble, CRC Press, 104th edn, 2023.

61 S. M. Boyt, *Synthesis of Novel Dihydropentalenes , Pentalenides and Hydropentalenides*, PhD Thesis, Bath, 2019.

62 S. You and M. Neuenschwander, New Pathways to Precursors of Pentalene, *Chimia*, 1996, **50**(1–2), 26, DOI: 10.2533/chimia.1996.24.

63 H. J. Sanderson, G. Kociok-Köhn, C. L. McMullin and U. Hintermair, Twinned *versus* Linked Organometallics - Bimetallic "Half-Baguette" Pentalenide Complexes of Rh(I), *Dalton Trans.*, 2024, **53**, 5881–5899, DOI: 10.1039/D3DT04325H.

64 R. Nozawa, J. Kim, J. Oh, A. Lamping, Y. Wang, S. Shimizu, I. Hisaki, T. Kowalczyk, H. Fliegl, D. Kim and H. Shinokubo, Three-Dimensional Aromaticity in an Antiaromatic Cyclophane, *Nat. Commun.*, 2019, **10**(1), 1–7, DOI: 10.1038/s41467-019-11467-4.

65 K. Hanida, J. Kim, N. Fukui, Y. Tsutsui, S. Seki, D. Kim and H. Shinokubo, Antiaromatic 1,5-Diaza-s-Indacenes, *Angew. Chem., Int. Ed.*, 2021, **60**(38), 20765–20770, DOI: 10.1002/ANIE.202109003.

66 H. Kawashima, S. Ukai, R. Nozawa, N. Fukui, G. Fitzsimmons, T. Kowalczyk, H. Fliegl and H. Shinokubo, Determinant Factors of Three-Dimensional Aromaticity in Antiaromatic Cyclophanes, *J. Am. Chem. Soc.*, 2021, **143**(28), 10676–10685, DOI: 10.1021/JACS.1C04348.

67 N. A. Jenek, A. Helbig, S. M. Boyt, M. Kaur, H. J. Sanderson, S. B. Reeksting, G. Kociok-Köhn, H. Helten and U. Hintermair, Understanding and Tuning the Electronic Structure of Pentalenides, *Chem. Sci.*, 2024, **15**(32), 12765–12779, DOI: 10.1039/D3SC04622B.

68 A. Stanger, Nucleus-Independent Chemical Shifts (NICS): Distance Dependence and Revised Criteria for Aromaticity and Antiaromaticity, *J. Org. Chem.*, 2006, **71**(3), 883–893, DOI: 10.1021/JO051746.

69 A. Stanger, G. Monaco and R. Zanasi, NICS-XY-Scan Predictions of Local, Semi-Global, and Global Ring Currents in Annulated Pentalene and s-Indacene Cores Compared to First-Principles Current Density Maps, *ChemPhysChem*, 2020, **21**(1), 65–82, DOI: 10.1002/CPHC.201900952.

70 N. D. Charistos, A. G. Papadopoulos, T. A. Nikopoulos, A. Muñoz-Castro and M. P. Sigalas, Canonical Orbital Contributions to the Magnetic Fields Induced by Global and Local Diatropic and Paratropic Ring Currents, *J. Comput. Chem.*, 2017, **38**(30), 2594–2604, DOI: 10.1002/JCC.24917.

71 M. H. Garner, J. T. Blaskovits and C. Corminboeuf, Double-Bond Delocalization in Non-Alternant Hydrocarbons Induces Inverted Singlet–Triplet Gaps, *Chem. Sci.*, 2023, **14**(38), 10458–10466, DOI: 10.1039/D3SC03409G.